Fatigue lifetime assessment of notched components under multiaxial variable amplitude loading based on a short crack growth concept

O. Hertel[1], M. Vormwald[2]

[1] Robert Bosch GmbH, CR/APM2, Postfach 300240, 70442 Stuttgart, Germany, olaf.hertel@de.bosch.com
[2] Technische Universität Darmstadt, Fachgebiet Werkstoffmechanik, Petersenstr. 12, 64287 Darmstadt, Germany, vormwald@wm.tu-darmstadt.de

ABSTRACT. *A short crack model originally proposed for multiaxial constant amplitude loading is extended and applied to cases of multiaxial variable amplitude loading. Load sequence influences that play an important role under variable amplitude loading are implemented based on some algorithms originally only proposed for uniaxial loading. Estimated Fatigue lives of unnotched tubular specimen and notched shaft under different in- and out-of-phase multiaxial constant and variable amplitude load histories are compared to experimental results. The comparison yields satisfying estimation accuracy for the presented short crack approach. Even the critical planes, planes of maximum crack growth or minimum crack growth life, respectively, are estimated with good agreement to experimental observations.*

INTRODUCTION

Mostly, the estimation of fatigue life of notched components under variable amplitude loading is based on experimental data that is derived under constant amplitude loading and by application of a certain damage accumulation rule. The estimation accuracy of such damage accumulation rule mainly depends on whether load sequence influences are taken into account or not. The most important load sequence effects are: mean stress rearrangement due to local elastic-plastic deformation, reduction of fatigue strength with accumulated damage and crack closure due to plastic deformation ahead of the crack tip.

Additional difficulties arise, if only experimental fatigue life data from unnotched smooth material specimens is available. Then a fatigue life estimation approach is needed, that transfers this data from smooth to notched specimen and accumulates the damage with respect to load sequence effects.

Within the current investigation a fatigue life estimation approach for multiaxial constant amplitude loading is applied to cases of variable amplitude loading. The approach is based on a short crack model proposed by Döring [1] and was already presented in previous papers [2, 3, 4]. There the short crack model was extended to qualitatively and quantitatively cover the geometrical size effect that is of importance for notched components. Within the current paper some extensions are proposed to deal with multiaxial variable amplitude loading.

EXPERIMENTAL INVESTIGATION

Most of the experimental results were obtained during an already completed DFG supported research program [5]. Within this research program fatigue lives of a tubular specimen and a notched specimen were investigated under combined tension/compression and torsion loading. The tubular specimens have an outer diameter of 41 mm and a wall thickness of 2.5 mm. The notched geometry is a round shaft with a shoulder fillet. The shaft diameters are 27 mm and 35 mm and the fillet radius is 1.4 mm (Fig. 1a). Both specimen types are made of an unalloyed fine grain steel S460N. Additionally there is a series of tubular specimens made of an aluminium alloy AW-5083. The Monotonic and cyclic material data of the two materials is shown in Table 1.

Table 1. Monotonic and cyclic material data

	E [N/mm²]	ν	$R_{p0.2}$ [N/mm²]	R_m [N/mm²]	A_5 [%]
S460N	208,500	0.3	500	643	26
AW-5083	68,000	0.33	169	340	20

	K' [N/mm²]	n'	σ_f' [N/mm²]	ε_f'	b	c	N_E
S460N	1115	0.161	969.6	0.281	-0.086	-0.493	$5 \cdot 10^5$
AW-5083	544	0.075	780.3	1.153	-0.114	-0.8614	$1 \cdot 10^6$

The tubular specimens are loaded under normal and shear strain control using a biaxial extensometer with a gage length of 12.5 mm. The ratio of normal strain amplitudes to shear strain amplitudes is set to 0.577, to get nearly identical distributions to the von Mises equivalent plastic strain under proportional loading. The notched specimens are loaded under force (F) and torque (M) control. The ratio between torsion and tension/compression net section stresses is set to 0.873 to get a ratio between local normal strains and local shear strains of approximately 0.577. The elastic notch factor for tension/compression loading is 2.45 and for torsion loading 1.56.

Several fatigue tests with in-phase and 90° out-of-phase constant amplitude loading (CA) and in-phase and 90° out-of-phase variable amplitude loading (VA) were carried out.

All tests were performed with a constant test frequency of 1 Hz and sinusoidal load signals. The 90° phase shift was realised by a 0.25 seconds retarded start of the shear strain/torque load signal. The phase shift was permanently controlled during the tests. The load spectra of the variable amplitude load histories are shown in Figure 1b. The load spectrum for the strain controlled tubular specimen has a linear shape and contains 4,256 load cycles. Small strain cycles with amplitudes lower than 20 % of the maximum strain amplitude are omitted, to reduce testing and calculation time. The load spectrum for the force/torque controlled tests at the notched specimen has a Gaussian shape and contains 10^5 cycles. Both load sequences have a mean R-ration of -1.

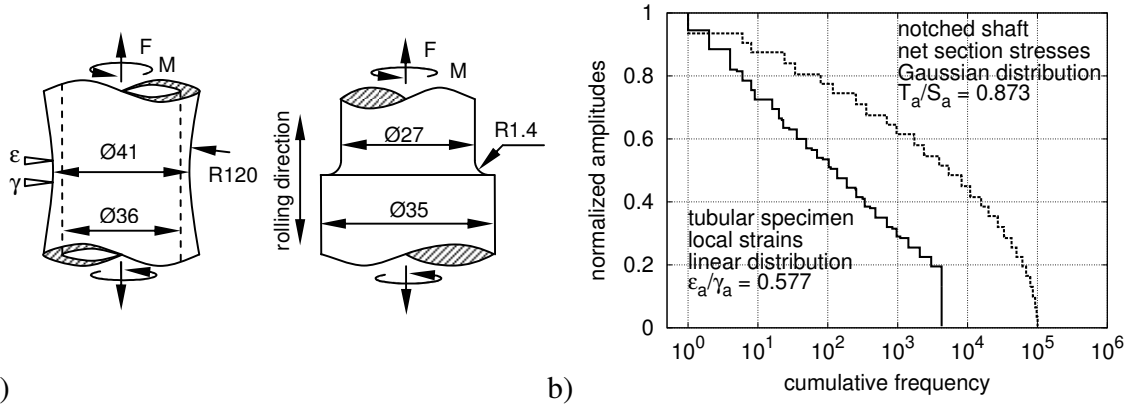

Figure 1. a) Geometry and b) load spectra tubular and notched specimen. (in mm)

The fatigue crack growth was observed with an optical microscope and by plastic replica technique (Fig. 4). The failure criterion is fulfilled if a surface crack length of 0.5 mm is reached. In most cases the fatigue life was determined by the growth of a single crack. If several cracks were initiated, the largest of them determines the fatigue life.

SHORT CRACK MODEL

Within the framework of the short crack model, the fatigue life is defined as crack growth life of a semi-elliptical surface crack (Fig. 2). The crack growth is assumed to be always planar. Therefore the short crack model is a critical plane model. The critical plane is defined as plane of maximum crack growth or minimum crack growth life, respectively. The crack growth starts from

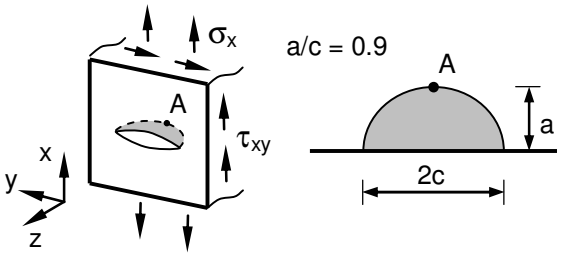

Figure 2. Semi-elliptical surface crack.

zero crack length and ends if a surface crack length 2*c* of 0.5 mm is reached. In contrast to [3, 4] a constant ratio of crack depth to crack length of *a/c*=0.9 is assumed. This is equal to the ratio of a semi-elliptical surface crack in a homogenous stress field under Mode I loading. Due to that simplification only the crack growth at the deepest point A of the surface crack has to be considered (Fig. 2).

Crack growth law

The crack growth law is a Paris-type power law based on effective ranges of cyclic J-Integral as defined by Wüthrich [6]. Please note that according to Wüthrich [6], in the following, the symbol Z is used instead of the symbol ΔJ. It is assumed that each crack opening mode (Mode I, II and III) independently contributes to the crack growth. Therefore no additional Mixed Mode criterion is necessary.

$$\frac{\mathrm{d}a}{\mathrm{d}n} = C \cdot {Z_{\mathrm{I,eff}}}^{m} + C \cdot {Z_{\mathrm{II,eff}}}^{m} + C \cdot {Z_{\mathrm{III,eff}}}^{m} \quad \text{with} \quad C = 10^{-5} \cdot \left(\frac{5 \cdot 10^{5}}{E} \cdot \frac{1}{\mathrm{mm}} \right)^{m} \tag{1}$$

The crack growth constant C is approximately determined based on [7]. The slope m is equal to the slope of the life-curve derived from strain-life test data if the effective strain energy density $\Delta W_{\mathrm{x,eff}}$ (Eq. 3) is plotted over cycles N to failure.

Following a proposal from Hoshide and Socie [8], the crack driving forces Z_{I}, Z_{II} and Z_{III} are approximated based on effective ranges of the associated elastic-plastic strain energy density:

$$Z_{\mathrm{I,eff}} = 2\pi {Y_{\mathrm{I,A}}}^{2} \Delta W_{\mathrm{x,eff}} \cdot a \quad Z_{\mathrm{II,eff}} = \frac{\pi}{1+\nu} {Y_{\mathrm{II,A}}}^{2} \Delta W_{\mathrm{xz}} U_{\mathrm{eff}} \cdot a \quad Z_{\mathrm{III,eff}} = \pi {Y_{\mathrm{III,A}}}^{2} \Delta W_{\mathrm{xy}} U_{\mathrm{eff}} \cdot a \tag{2}$$

Herein, $Y_{\mathrm{I,A}}$=0.70 $Y_{\mathrm{II,A}}$=0.62 and $Y_{\mathrm{III,A}}$=0.58 are geometry influence functions for the deepest point of a semi-elliptical surface crack with constant *a/c* ratio of 0.9, according to the stress intensity factor concept and theory of linear elasticity. $\Delta W_{\mathrm{x,eff}}$ is the part of the elastic-plastic strain energy density that is composed during an opened crack by integrating stresses normal to the crack face over the corresponding strains. The integration is performed along the falling hyteresis branch. The points of crack opening and closure are calculated based on an extended Newman-formula mentioned in [1]. It is assumed, that crack opening and crack closure occur at the same normal strain level. ΔW_{xy} is the part of the strain energy density that is composed out of the surface parallel shear stresses and strains in the crack plane. According to the definition of Brown and Miller [9], this part of strain energy density corresponds to “Case A” cracks. “Case B” cracks, which are inclined to the surface, are considered by $Z_{\mathrm{II,eff}}$ and ΔW_{xz}.

$$\Delta W_{\mathrm{x,eff}} = \int_{\varepsilon_{\mathrm{x,max}}}^{\varepsilon_{\mathrm{x,cl}}} \left(\sigma_{\mathrm{x}} - \sigma_{\mathrm{x,max}}\right) \mathrm{d}\varepsilon_{\mathrm{x}} \,;\; \Delta W_{\mathrm{xy}} = \int_{\gamma_{\mathrm{xy,max}}}^{\gamma_{\mathrm{xy,min}}} \left(\tau_{\mathrm{xy}} - \tau_{\mathrm{xy,max}}\right) \mathrm{d}\gamma_{\mathrm{xy}} \,;\; \Delta W_{\mathrm{xz}} = \int_{\gamma_{\mathrm{xz,max}}}^{\gamma_{\mathrm{xz,min}}} \left(\tau_{\mathrm{xz}} - \tau_{\mathrm{xz,max}}\right) \mathrm{d}\gamma_{\mathrm{xz}} \quad (3)$$

The factor U_{eff} in Eq. 2 is between 0 and 1 and incorporates indentation and friction of the crack faces and therefore micro-structural effects on one hand, and the influence of a normal stress on shear crack growth on the other hand. The factor is set equal to the ratio of the crack tip sliding displacement of a Mode II Dugdale model [10] with and without friction stresses on the crack faces:

$$U_{eff} = \frac{\Delta CTSD_{fric}}{\Delta CTSD} = \ln\left(\cos\left(\frac{\pi}{2} \cdot \frac{\Delta\tau/2 - \tau_{fric}}{\tau_F - \tau_{fric}}\right)^{-1}\right) \Bigg/ \ln\left(\cos\left(\frac{\pi}{2} \cdot \frac{\Delta\tau/2}{\tau_F}\right)^{-1}\right) \quad (4)$$

$\Delta\tau$ represents the shear stress range $\Delta\tau_{\mathrm{xy}}$ or $\Delta\tau_{\mathrm{xz}}$, respectively. The shear yield stress τ_{F} and the friction stress on the crack surface τ_{fric} are defined as follows.

$$\tau_{\mathrm{F}} = \sigma_F / \sqrt{3} \quad \sigma_F = \left(R'_{p0.2} + R_m\right)/2 \quad \tau_{\mathrm{fric}} = \left\langle \tau_{\mathrm{act}} - \mu \cdot \sigma_{\mathrm{n}} \right\rangle \quad (5)$$

Herein σ_{n} is the mean normal stress over one whole shear strain cycle. τ_{act} is a constant friction stress due to crack face indentation and μ is a friction coefficient. These two parameters are fitted to experimental fatigue life data under cyclic shear stress or strain with superposed static normal stress or strain, respectively.

The crack growth of micro structural short cracks is strongly influenced by the microstructure. Especially the crack growth rate of micro structural short crack is higher than the crack growth rate of long cracks with comparable ΔK. All micro structural influences are crudely summarised by introducing an intrinsic crack depth a_0. The intrinsic crack depth a_0 is simply added to the actual crack depth a. It is calculated from the strain-life-curve by backward integration of the crack growth law. For the fine grain steel S460N the intrinsic crack depth a_0 is 17 µm and for the aluminium alloy AW-5083 a_0 is 24 µm. This is approximately equal to the double of the mean grain size.

Crack growth threshold

Crack growth is only calculated for cycles with $Z_{\mathrm{I,eff}}$, $Z_{\mathrm{II,eff}}$ or $Z_{\mathrm{III,eff}}$ larger than the short crack growth threshold. The short crack growth threshold $Z_{\mathrm{eff,th,SC}}$ is in general lower than the crack growth threshold for long cracks $Z_{\mathrm{eff,th,LC}}$. It is dependent from the crack depth a and tends towards the long crack threshold if cracks get larger.

$$Z_{\text{eff,th,SC}} = Z_{\text{eff,th,LC}} \cdot \frac{a}{a + a^*} \quad \text{with} \quad a^* = \frac{Z_{\text{eff,th,LC}}}{2\pi {Y_{I,A}}^2 \Delta W_{x,eff,E}} \quad \text{and} \quad Z_{\text{eff,th,LC}} = \frac{E}{5 \cdot 10^6} \cdot \text{mm} \quad (6)$$

The value a^* is adjusted, so that in case of a micro structural short crack the fatigue strength of the material is obtained. Here the term fatigue strength means that no surface cracks can be observed after a large but finite number of load cycles (e.g. $2 \cdot 10^6$). The value of a^* can be calculated based on the long crack threshold value and the effective strain energy density (Eq. 2) on the level of fatigue strength. The crack growth threshold for long cracks expressed in Z_{eff} is approximated based on [7]. All material dependent model parameters of the short crack model are summarized in Table 2.

Table 2. Material dependent model parameters of the short crack model

	m	$C \left[\frac{\text{mm}}{\text{cycle}} \cdot (\text{N/mm})^{-m} \right]$	a_0 [µm]	μ [-]	τ_{act} [N/mm²]	$Z_{\text{eff,th,LC}}$ [N/mm]
S460N	1.73	$4.53 \cdot 10^{-5}$	17	0.1	0	0.042
AW-5083	1.69	$2.90 \cdot 10^{-4}$	24	0.1	68	0.014

Local elastic-plastic stresses and strains

The local elastic-plastic stresses and strains under multiaxial constant and variable amplitude loading are calculated based on an advanced plasticity model proposed by Döring [11]. For the notched shaft additionally a modified multiaxial approximation procedure originally proposed by Köttgen et. al. [12, 13] is used to derive the elastic-plastic notch root strains from the applied loads.

Load sequence influences

Dealing with variable amplitude loading several load sequence influences have to take into account. The most important load sequence influences are mean stress rearrangement due to local elastic-plastic deformation, reduction of fatigue strength with accumulated damage or crack depth and crack closure due to plastic deformation ahead of the crack tip.

Within the framework of the proposed short crack model all these load sequence influences are explicitly included. By simulating the local elastic-plastic strain and stress history the mean stress rearrangement has been already taken into account. The crack depth dependent reduction of the fatigue strength is realised by Eq. 9 that defines a crack length dependent short crack growth threshold. Load sequence effects due to plastic deformation ahead of the crack tip are modelled according to Vormwald [7]. The crack opening/closure strain of large load cycles influences the crack opening/closure strain of following smaller load cycles. Additionally a retardation of this effect with increasing crack depth or damage, respectively, is modelled.

Cycle counting and damage accumulation
Damaging load cycles are identified by rainflow counting of the strain time history. Each strain component ε_x, γ_{xy} and γ_{xz} is counted separately. If a cycle is identified, the corresponding range of effective strain energy density (Eq. 3) and the cyclic J-Integral value (Eq. 2) are calculated. If this value is higher than the short crack threshold (Eq. 6), then the corresponding crack growth increment is calculated based on Eq. 1 and is added to the actual crack depth. Because of load sequence influences the whole load time history is processed 3 times. If thereafter the crack length is still below 0.5 mm, the integration of the crack growth law (Eq. 1) is continued based on ranges of effective strain energy density values that were obtained during the last repetition of the load time history.

Statistical size effect
The highly stressed surface of the notched specimen is similar to that of a common material specimen. Therefore the statistical size effect is neglected. In contrast, the highly stressed surface of the hollow tube specimen (A_{tube}=1495 m²) is approximately 22 times larger than that of a common material specimen (A_{ref}=67 mm²). Due to that fact the statistical size effect has to be considered. The experimental observed statistical support factor (vertical shift of stress-life-curve) for the tubular specimen is 0.94 [14]. The statistical support factor is taken into account by a higher intrinsic crack depth a_0. It is calculated on the basis of a shifted strain-life curve by backward integration of the crack growth law.

RESULTS AND DISCUSSION

The experimentally observed and calculated fatigue lives for the tubular specimen are shown in Fig. 3. In case of in-phase constant amplitude loading the experimentally observed and calculated fatigue lives are in very good agreement. This holds true for both materials the fine grain steel S460N and the aluminium alloy AW-5083. The experimentally observed fatigue crack growth occurs mainly in planes of maximum normal strain between 20° and 30° to the specimen axis (Fig. 4). The calculated plane of minimum crack growth life is 25° to the specimen axis, which is again in good accordance with experimental results.

Under 90° out-of-phase constant amplitude loading and for the aluminium alloy the short crack model yields approximately a factor of 2 longer fatigue lives than under in-phase loading. For the fine grain steel no influence of phase shift is calculated. This is not found experimentally. The experiments show no influence of phase shift for the aluminium alloy and shorter fatigue lives for the fine grain steel. A look onto the crack angles shows the complexity of the out-of phase loading. The calculated crack angle for the aluminium alloy divers from the experimental result as it is expected if one looks onto the calculated

fatigue lives. But for the fine grain steel the calculated and experimental crack angle are in good agreement. Despite the fact, that the calculated fatigue live are too long.

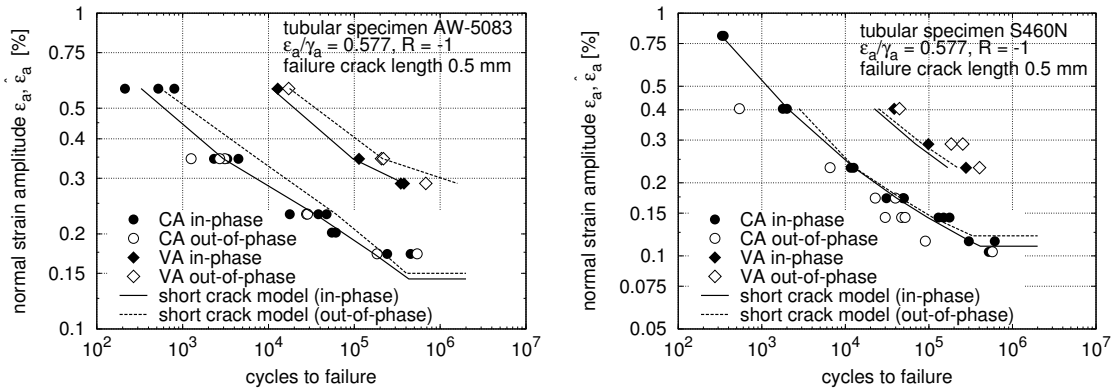

Figure 3. Experimentally observed [14] and calculated constant and variable amplitude strain life curves, tubular specimen, aluminium alloy AW-5083 and steel S460N.

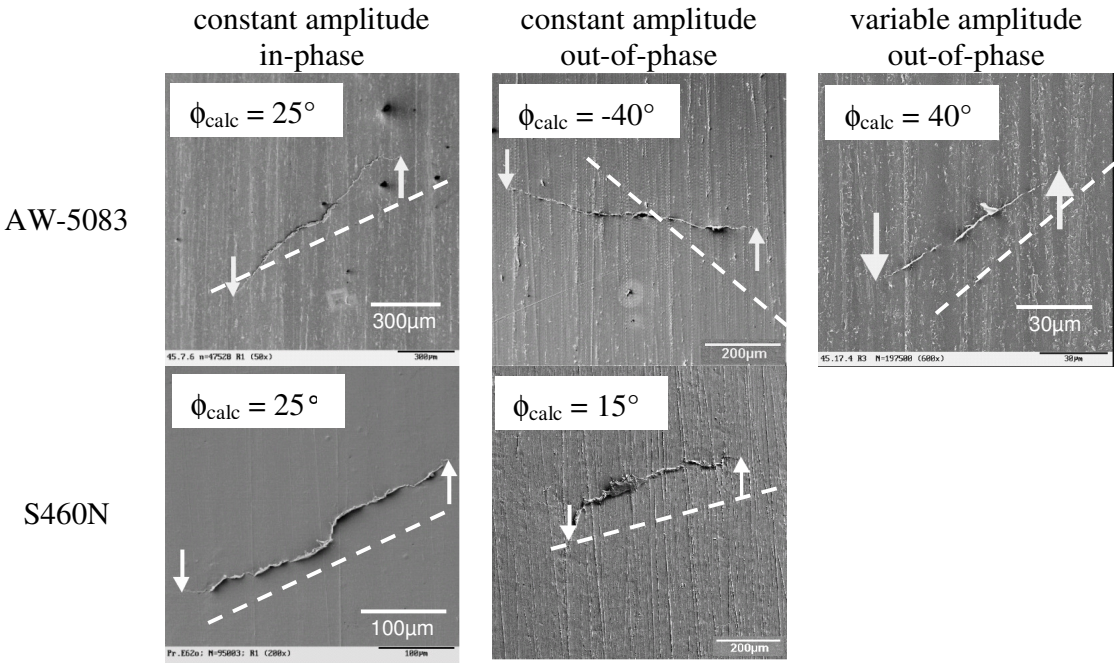

Figure 4. Experimentally observed [14] and calculated crack angles, tubular specimen.

Under variable amplitude loading the 90° phase shift experimentally results in longer lives compared to in-phase loading. This effect is more pronounced for the aluminium alloy than for the fine grain steel. The calculated fatigue lives from the short crack model show the same tendency and are in good agreement with the experimental observations. For the fine grain steel with larger plastic deformation the short crack model is conservative. Unfortunately only the experimentally observed crack angle for the aluminium alloy and out-phase variable amplitude loading is available. The calculated crack plane for that case is nearly the same (see Fig. 4).

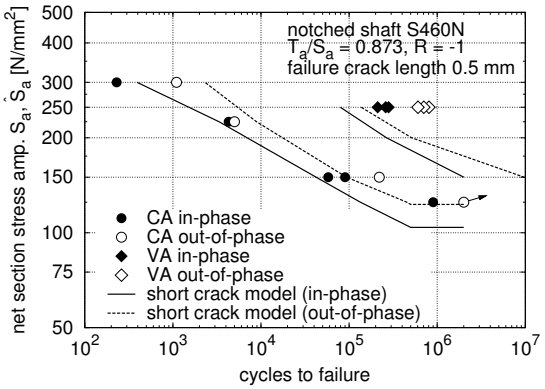

Figure 5. Experimentally observed and calculated constant amplitude S-N-curves and variable amplitude life curves for notched steel specimen.

The results for the notched specimen are shown in Fig. 5. The calculated S-N-curves for in-phase and 90° out-of-phase loading are in good agreement with the experimental results. Some differences between calculation and experiments exist in the region between 100 N/mm² and 150 N/mm². Here the short crack model seems to be conservative. Because the most damaging parts of the load spectrum are within this region, the conservative behaviour is also reflected in the calculated life curves for variable amplitude loading. Despite that, the accuracy of the short crack model is quite satisfying.

SUMMARY

Within the current investigation a short crack model originally proposed by Döring [1] for multiaxial constant amplitude loading was extended and successfully applied to cases of variable amplitude loading. The extended short crack model now accounts for the most important load sequence influences, which are local mean stress rearrangement, reduction of fatigue strength with accumulated damage and crack closure due to plastic deformations

ahead of the crack tip. Those effects are described based on algorithms originally proposed by Vormwald [7] for uniaxial loading. These algorithms are transferred to multiaxial loading based on the concept of critical planes.

The comparison of calculated fatigue lives with experimental observations yields a satisfying accuracy. Even calculated critical planes, planes of maximum crack growth, are in good agreement with experimental observations. The results for 90° out-of-phase loading show that not all of the complex damage mechanisms are understood and implemented correctly. Especially the interaction between Mode I crack growth on the one hand and Mode II and Mode III crack growth on the other hand needs further investigations.

ACKNOWLEDGEMENTS

The authors would like to express their sincere gratitude to the "Deutsche Forschungs-gemeinschaft" for financial support without which this study would not have been possible.

REFERENCES

1. Döring, R., Hoffmeyer, J., Seeger T., Vormwald, M. (2006) *Int. J. Fatigue* **28**, 972-982.
2. Jiang, Y., Hertel, O., Vormwald, M., (2007) *Int. J. Fatigue* **29**, 1490-1502.
3. Hertel, O. and Vormwald, M. (2007) In: *Proceedings of ICMFF 8*, Sheffield.
4. Vormwald, M. and Hertel, O. (2008) *Mat.-wiss. u. Werkstofftech.* **39**, 702-710.
5. Hoffmeyer, J., Döring, R., Seeger, T., Vormwald, M. (2006) *Int. J. Fatigue* **28**, 508-520
6. Wüthrich, C. (1982) *Int. J. Fract.* **20**, R35-R37.
7. Vormwald, M. (1989) PhD-Thesis, Technische Universität Darmstadt, Germany.
8. Hoshide, T. and Socie, D.F. (1987) *Engng. Fract. Mech.* **26**, 841-850.
9. Brown, M.W., Miller, K.J. (1973) In: *Proc. Inst. Mech. Engrs.* **187**, 745-755.
10. Becker, W., Gross, D. (1988) *Int. J. Fract.* **37**, 163-170.
11. Döring, R., Hoffmeyer, J., Seeger, T., Vormwald, M. (2006) *Comp. Mat. Sci.* **28**, 972-982.
12. Köttgen, V.B., Barkey, M.E., Socie, D.F. (1995) *Fat. Fract. Engng. Mater. Struct.* **18**, 981-1006.
13. Hertel, O., Vormwald, M., Seeger, T., Döring, R., Hoffmeyer, J. (2005) *Materials Testing MP* **47**, 268-277.
14. Hoffmeyer, J. (2004) PhD-Thesis, Technische Universität Darmstadt, Germany.